

NATIONAL AERONAUTICS AND SPACE ADMINISTRATION

PROPOSED JOURNAL ARTICLE

LAMINAR SLIP FLOW IN A FLAT DUCT OR A ROUND
TUBE WITH UNIFORM WALL HEAT TRANSFER

by Robert M. Inman

Lewis Research Center
Cleveland, Ohio

GPO PRICE \$ _____

CFSTI PRICE(S) \$ _____

Hard copy (HC) 2.00Microfiche (MF) .50

FACILITY FORM 602

N66-18390

(ACCESSION NUMBER)

37

(PAGES)

TMX 56055

(NASA CR OR TMX OR AD NUMBER)

(THRU)

1

(CODE)

33

(CATEGORY)

ff 653 July 65

Prepared for

International Journal of Heat and Mass Transfer

September 22, 1964

64-11

~~AVAILABLE TO NASA AND NASA CENTERS ONLY~~

LAMINAR SLIP FLOW IN A FLAT DUCT OR A ROUND
TUBE WITH UNIFORM WALL HEAT TRANSFER

by Robert M. Imman

Lewis Research Center
National Aeronautics and Space Administration
Cleveland, Ohio

ABSTRACT

N66-18390

An analysis was made to determine the effects of low-density phenomena on the heat-transfer characteristics for laminar flow in a parallel-plate channel (flat duct) or in a circular tube with uniform wall heat flux. Consideration was given to the slip-flow regime, wherein the major rarefaction effects are displayed as velocity and temperature jumps at the conduit walls. The results obtained apply along the entire length of the conduit, that is, in the thermal entrance region as well as far downstream. The solutions contain a series expansion, and analytical expressions for the complete set of eigenvalues and eigenconstants for this problem are presented. The results give the wall temperatures, Nusselt numbers, and thermal entrance lengths for the conduits for various values of the rarefaction parameters.

NOMENCLATURE

Author

a	accommodation coefficient
C_m	coefficient in series for temperature distribution in parallel-plate channel
C_n	coefficient in series for temperature distribution in circular tube
C_p	specific heat at constant pressure

REPRODUCED FROM THE NASA LITERATURE SERVICE AND NASA CENTERS ONLY

D_m	coefficient defined by equation (32)
D_n	coefficient defined by equation (57)
D_T	thermal diameter, $8L/\sigma$
d	tube diameter, $2r_0$
E_σ	constant defined in equation (31)
$f(\eta)$	dimensionless velocity for parallel-plate channel, $u(\eta)/\bar{u}$
$f(\omega)$	dimensionless velocity for circular tube, $u(\omega)/\bar{u}$
$G(\eta)$	transverse temperature distribution in fully developed region for parallel-plate channel
g	specular reflection coefficient
$H(\omega)$	transverse temperature distribution in fully developed region for circular tube
h	heat-transfer coefficient, $q/(t_w - t_b)$
I_1, \tilde{I}_1	value of definite integral, equation (34) for parallel-plate channel, equation (59) for round tube
J_1	Bessel function of first kind and first order
L	half distance between plates
l	mean free path
M	constant defined by equation (60)
N	constant defined by equation (61)
Nu	Nusselt number, hD_T/κ or hd/κ
Pr	Prandtl number, $\mu C_p/\kappa$
p	static pressure
q	rate of heat flux per unit area from wall to fluid
R	transverse or radial distribution function

Re	Reynolds number, $2\rho uL/\mu$ for parallel-plate channel, $\rho u d/\mu$ for circular tube
R_g	gas constant
R_m	eigenfunctions of equation (14) for parallel-plate channel
R_n	eigenfunctions of equation (43) for circular tube
r	radial coordinate
r_0	tube radius
t	temperature
t_g	gas temperature adjacent to wall
u	velocity
x	axial coordinate
y	transverse coordinate

Greek symbols:

α	dimensionless velocity slip coefficient, $\xi_u/2L$ or ξ_u/d
β_m	$\lambda_m^{1/2} I_1$
β_n	$\lambda_n^{1/2} I_1$
γ	ratio of specific heats
ζ	dimensionless coordinate, $x/2L$ or x/r_0
η	dimensionless coordinate, $oy/2L$
κ	gas thermal conductivity
λ	separation constant
λ_m	eigenvalues of equation (14) for parallel-plate channel
λ_n	eigenvalues of equation (43) for round tube
μ	absolute viscosity
ξ_t	temperature-jump coefficient
ξ_u	velocity-slip coefficient

ρ	gas density
σ	symmetry number
ϕ	rarefaction parameter, $\mu \sqrt{R_g t} / 2pL$ or $\mu \sqrt{R_g t} / pd$
ψ	dimensionless quantity, $RePr/\sigma^2$ for parallel-plate channel, $RePr/4$ for circular tube
ω	dimensionless coordinate, r/r_0

Subscripts:

b	bulk condition of gas
d	fully developed region
d,c	fully developed region for continuum flow
e	entrance region
i	gas entering channel, $x = 0$
s	slip condition at wall
w	wall
0	heated section entrance, $x = 0$

Superscript:

-	average value
---	---------------

INTRODUCTION

In recent years, considerable interest has developed in the study of the fluid-flow and heat-transfer characteristics of rarefied gases. This interest has been stimulated by the increasing frequency of low-density-environment applications and the advent of space flight. Only very recently has attention been directed to the problem of heat transfer to rarefied gas flow in conduits.

Of particular interest in internal, rarefied gas-flow studies has been the problem of laminar forced-convection heat transfer in conduits under

slip-flow conditions [1 and 2]. The essential simplifications introduced in these investigations to obtain analytical solutions are fully established temperature profiles and fully developed velocity distributions.

The present investigation is concerned with the more general problem of determining the heat-transfer characteristics along the entire length of the conduit, that is, in the thermal entrance region as well as far downstream, for laminar slip flow in a parallel-plate channel (often referred to as a "flat duct") or in a circular tube with uniform wall heat flux.

In the section FLOW IN PARALLEL-PLATE CHANNEL is considered the problem of slip flow of a rarefied gas in a parallel-plate channel with uniform wall heat flux at one or at both walls. Both heating arrangements are frequently encountered in practical applications. The problem of slip flow in a circular tube with uniform wall heat flux is discussed in the section FLOW IN CIRCULAR TUBE.

FLOW IN PARALLEL-PLATE CHANNEL

The coordinate systems for the problems under study are shown in Fig. 1. A slightly rarefied gas flows in the positive x -direction with a fully established velocity profile. Up to a point ($x = 0$) the channel walls and gas are isothermal at temperature t_1 . After this point a uniform wall heat flux is applied. It is desired to determine the temperature distribution and the variation in the heat-transfer coefficient along the entire length of the channel.

It is convenient to place the plane $y = 0$ at the plane of symmetry, that is, at the middle of the duct in the case of heating of both walls at

$y = \pm L$ (Fig. 1(a)) and at the insulated wall in the case of heating from one side at $y = +2L$ (Fig. 1(b)). Both cases are included in the following development by defining a symmetry number σ , which is also the number of heating surfaces [3].

Before the energy equation can be solved, the gas velocity distribution must be known. This distribution was investigated in [4]. The use of the results leads to the dimensionless velocity profiles $u(\eta)/\bar{u}$ as

$$f(\eta) = (3/2)(1 - \eta^2 + 4\alpha)/(1 + 6\alpha) \quad \sigma = 2 \quad (1)$$

$$f(\eta) = 6(\eta - \eta^2 + \alpha)/(1 + 6\alpha) \quad \sigma = 1 \quad (2)$$

where $\alpha \equiv \xi_u/2L$. The slip coefficient ξ_u is given by the expression [5]

$$\xi_u = [(2 - g)/g]\lambda \quad (3)$$

where λ is the mean free path and g is the specular reflection coefficient. The relation between the average velocity and the slip velocity is easily obtained as

$$u_s/\bar{u} = 6\alpha/(1 + 6\alpha) \quad \sigma = 1, 2 \quad (4)$$

The starting point of the heat-transfer analysis is the differential equation for convective heat transfer in the parallel-plate channel flow with fully established velocity profile. With the gas properties assumed constant, the heat conduction in the flow direction compared with that in the transverse y -direction assumed negligible, and the viscous dissipation assumed negligible, the equation can be written in the form

$$\rho C_p u (\partial t / \partial x) = \kappa (\partial^2 t / \partial y^2) \quad (5)$$

Equation (5), written in terms of dimensionless variables, becomes

$$\psi F(\eta)(\partial t / \partial \zeta) = (\partial^2 t / \partial \eta^2) \quad (6)$$

The boundary conditions are as follows:

Uniform wall heat flux:

$$\partial t / \partial \eta = (2L/\sigma)(q/k) \text{ at } \eta = 1, \zeta \geq 0$$

Symmetry:

$$\partial t / \partial \eta = 0 \text{ at } \eta = 0$$

Specified entrance temperature:

$$t = t_1 \text{ at } \zeta = 0$$

When the wall heat flux is uniform, it is known that for very large values of x there is a fully developed thermal situation characterized by a linear rise in the temperature at all points in the cross section along the channel; that is,

$$(\partial t_d / \partial x) = (\sigma q / \text{RePr}k) \quad \sigma = 2, 1 \quad (7)$$

Equation (7) can be written alternatively as

$$(t_d - t_1) / (2L/\sigma)(q/k) = \sigma^2(x/2L) / \text{RePr} + G(\eta) \quad (8)$$

The function $G(\eta)$ for each value of σ is

$$G(\eta) = [(3/4)\eta^2 - (1/8)\eta^4 - (39/280)] + [-(1/4)\eta^2 + (1/8)\eta^4 - (13/280)](u_g/\bar{u}) + [2/105](u_g/\bar{u})^2 \quad \sigma = 2 \quad (9a)$$

$$G(\eta) = [\eta^3 - (1/2)\eta^4 - (9/70)] + [(1/2)\eta^4 - \eta^3 + (1/2)\eta^2 - (3/70)](u_g/\bar{u}) + [1/210](u_g/\bar{u})^2 \quad \sigma = 1 \quad (9b)$$

The details of the analysis for $G(\eta)$ are omitted in the present study but may be found in [4]. The first quantity in brackets on the right side of (9a) and (9b) represents the usual transverse temperature distribution for continuum flow conditions, while the second and third quantities in brackets are connected with one effect of gas rarefaction, namely, that of velocity jump.

Determining the solution in the entrance region is convenient if a difference temperature t_e is defined as

$$t_e(\zeta, \eta) = t(\zeta, \eta) - t_d(\zeta, \eta) \quad (10)$$

Then t_e must satisfy the relation

$$\psi f(\eta) (\partial t_e / \partial \zeta) = \partial^2 t_e / \partial \eta^2 \quad (11)$$

with boundary conditions

$$\partial t_e / \partial \eta = 0 \quad \text{at} \quad \eta = 0 \quad \text{and} \quad \eta = 1 \quad (12)$$

The solution of (11) that will satisfy (12) can be found by using a product solution that leads to a separation of variables. This solution will have the form

$$t_e / (2L/\sigma)(q/k) = \sum_{m=1}^{\infty} C_m R_m(\eta) \exp[-\sigma^2 \lambda_m (x/2L)/\text{RePr}] \quad (13)$$

where λ_m and R_m are, respectively, the eigenvalues and eigenfunctions of the Sturm-Liouville problem:

$$\left. \begin{aligned} (d^2 R / d\eta^2) + \lambda f(\eta) R &= 0 \\ dR / d\eta &= 0 \quad \text{at} \quad \eta = 0 \quad \text{and} \quad \eta = 1 \end{aligned} \right\} \sigma = 2, 1 \quad (14)$$

The coefficients C_m in (13) are determined so as to satisfy the boundary condition at the entrance to the heated section $\zeta = 0$:

$$t_e(0, \eta) / (2L/\sigma)(q/k) = -G(\eta) = \sum_{m=1}^{\infty} C_m R_m(\eta) \quad (15)$$

This result together with the orthogonality property of the eigenfunctions leads to

$$\begin{aligned} C_m &= - \int_0^1 G(\eta) f(\eta) R_m(\eta) d\eta / \int_0^1 f(\eta) R_m^2(\eta) d\eta \\ &= \int_0^1 G(\eta) f(\eta) R_m(\eta) d\eta / [R(\eta) \partial^2 R / \partial \eta^2 \frac{\partial \lambda}{\partial \eta}]_{\eta=1, \lambda=\lambda_m} \quad \sigma = 2, 1 \end{aligned} \quad (16)$$

The integral in (16) can be evaluated by substituting $G(\eta)$ from (9a) or (9b) and $f(\eta)$ from (1) or (2), integrating by parts, and utilizing (14). The final result is identical for both cases:

$$C_m = 1/(\lambda \partial^2 R / \partial \eta \partial \lambda)_{\eta=1, \lambda=\lambda_m} \quad \sigma = 2, 1 \quad (17)$$

The complete solution for the temperature that applies in both the entrance and the fully developed regions is found by adding the solutions for t_d and t_e .

A result of practical interest is the longitudinal variation of wall temperature t_w corresponding to a uniform wall heat flux. Before the wall temperature variation can be determined, however, it is necessary to consider another effect of gas rarefaction that enters through the thermal boundary condition at the wall, which permits a jump between the surface temperature t_w and the adjacent gas temperature t_g [5]:

$$t_g - t_w = -\xi_t (\partial t / \partial y)_{y=2L/\sigma} \quad (18)$$

where ξ_t represents a temperature-jump coefficient related to other properties of the system by

$$\xi_t = [(2 - a)/a][2\gamma/(\gamma + 1)](1/Pr) \quad (19)$$

For uniform wall heat flux,

$$(\partial t / \partial y)_{y=2L/\sigma} = [(\partial t_d / \partial y) + (\partial t_e / \partial y)]_{y=2L/\sigma} = (q/k)$$

so that the temperature jump at the wall can be written

$$t_g - t_w = -(2L/\sigma)(q/k)[\sigma(\xi_t/2L)] \quad (20)$$

Combining (8) and (13) in accordance with (10), setting $\eta = 1$, and then combining the result with (20) yield

$$(t_w - t_1)/(2L/\sigma)(q/k) = \sigma^2(x/2L)/RePr + G(1) + \sigma(\xi_t/2L) + \sum_{m=1}^{\infty} C_m R_m(1) \exp[-\sigma^2 \lambda_m(x/2L)/RePr] \quad (21)$$

For a uniform wall heat flux, the bulk temperature $t_b(x)$ is given by

$$t_b = t_i + \sigma^2 [(2L/\sigma)(q/k)(x/2L)/\text{RePr}] \quad (22)$$

Combining (21) and (22) yields

$$(t_w - t_b)/(2L/\sigma)(q/k) = G(1) + \sigma(t_t/2L) + \sum_{m=1}^{\infty} C_m R_m(1) \exp[-\sigma^2 \lambda_m(x/2L)/\text{RePr}] \quad (23)$$

Then, for the fully developed situation ($x \rightarrow \infty$),

$$(t_w - t_b)_d / (2L/\sigma)(q/k) = G(1) + \sigma(t_t/2L) \quad (24)$$

Dividing (23) by (24) yields the important ratio

$$(t_w - t_b)/(t_w - t_b)_d = \left\{ G(1) + \sigma(t_t/2L) + \sum_{m=1}^{\infty} C_m R_m(1) \exp[-\sigma^2 \lambda_m(x/2L)/\text{RePr}] \right\} / [G(1) + \sigma(t_t/2L)] \quad (25)$$

Equation (25) can be evaluated once numerical values of λ_m , $R_m(1)$, and C_m have been obtained for given values of α or u_m/\bar{u} .

The Nusselt number may be determined from the definition of a thermal diameter D_T , which depends on the area of the heating surface [3]. For the present analysis, $D_T = 8L/\sigma$. Then, when this definition is applied,

$$\text{Nu} \equiv hD_T/k = [q/(t_w - t_b)](8L/\sigma k)$$

When (23) is used,

$$\text{Nu} = 4 \left\{ G(1) + \sigma(t_t/2L) + \sum_{m=1}^{\infty} C_m R_m(1) \exp[-\sigma^2 \lambda_m(x/2L)/\text{RePr}] \right\} \quad (26)$$

It is of interest to examine the behavior of the Nusselt number at the entrance of the heated section ($x = 0$) and also in the fully developed region ($x \rightarrow \infty$). At the entrance,

$$Nu_0 = 4 \left/ \left[G(1) + \sigma(\xi_t/2L) + \sum_{m=1}^{\infty} C_m R_m(1) \right] \right.$$

From (15), however, setting $\eta = 1$ yields

$$G(1) = - \sum_{m=1}^{\infty} C_m R_m(1)$$

so that

$$Nu_0 = 4/\sigma(\xi_t/2L) \quad \sigma = 2, 1 \quad (27)$$

In the absence of a temperature-jump effect, the local Nusselt number starts with $Nu_0 \rightarrow \infty$. With a temperature jump, however, the local Nusselt number commences with a finite value given by (27). The effect of the number of heating surfaces enters through the symmetry number σ .

When (26) is used, the fully developed Nusselt number is determined as

$$Nu_d = 4/[G(1) + \sigma(\xi_t/2L)] \quad \sigma = 2, 1 \quad (28)$$

The fully developed Nusselt number becomes for each case

$$Nu_d = (140/17) / [1 - (6/17)(u_g/\bar{u}) + (2/51)(u_g/\bar{u})^2 + (70/17)(\xi_t/2L)] \quad \sigma = 2 \quad (29a)$$

$$Nu_d = (140/13) / [1 - (3/26)(u_g/\bar{u}) + (1/78)(u_g/\bar{u})^2 + (35/13)(\xi_t/2L)] \quad \sigma = 1 \quad (29b)$$

In the absence of rarefaction effects, the fully developed Nusselt number

$Nu_{d,c}$ has the value $140/17 = 8.23$ ($\sigma = 2$) or $140/13 = 10.77$ ($\sigma = 1$).

From (29a) or (29b), it is clear that the effects of velocity jump ($u_g \neq 0$) would tend to increase the Nusselt number, while the temperature jump would act to decrease the Nusselt number. Similar results have been observed in the case of circular-tube slip flow [1,2].

Numerical values of the entrance Nusselt number (27) have been

evaluated as functions of the parameter $\mu\sqrt{R_g t}/2pL$ and related to the mean free path l by the relation [5] $\mu\sqrt{R_g t}/2pL = \sqrt{2/\pi} (l/2L)$. The values are plotted in Fig. 2. The values for γ and Prandtl number are representative of air and most diatomic gases. Fully developed Nusselt numbers as given by (29) have been evaluated as a function of the parameter $\mu\sqrt{R_g t}/2pL$ and are plotted in Fig. 3 for $\gamma = 1.4$, $Pr = 0.73$, $g = 1$, and $a = 1.0$ and 0.4 in the form of the ratio $Nu_d/Nu_{d,c}$ where $Nu_{d,c}$ is the appropriate fully developed continuum value. The effect of gas rarefaction is always to decrease the value of the Nusselt number below its continuum value, the result being more pronounced for two-sided heating than for one-sided heating.

The dimensionless wall-to-bulk temperature difference $(t_w - t_b)/(t_w - t_b)_d$, (25), and the local Nusselt number Nu , (26), can be evaluated along the entire duct length as soon as the eigenvalues λ_m , eigenfunctions $R_m(\eta)$, and series coefficients c_m have been determined. The function $R_m(\eta)$ is the solution of (14):

$$\begin{aligned} (d^2R/d\eta^2) + \lambda f(\eta)R &= 0 \\ dR/d\eta &= 0 \quad \text{at } \eta = 0 \quad \text{and } \eta = 1 \end{aligned} \quad \sigma = 2, 1 \quad (30a)$$

The normalization convention

$$R(0) = 1 \quad (30b)$$

is also used.

Asymptotic expressions for the eigenvalues λ_m and constants c_m and $R_m(1)$ for both the case $\sigma = 2$ and the case $\sigma = 1$ are derived in [4] and the results are presented as follows:

$$\beta_m \tan \beta_m = \left[\sqrt{4\alpha} + (1 + 4\alpha) \sin^{-1}(1/\sqrt{1 + 4\alpha}) \right] / 2\sigma(4\alpha)^{3/2} \equiv E_\sigma \quad (31)$$

$$D_m \equiv C_m R_m(1) = -8\alpha / [E_\sigma + 1 + (\beta_m^2/E_\sigma)] \quad (32)$$

where

$$\beta_m \equiv \sqrt{\lambda_m} I_1 \quad (33)$$

$$I_1 \equiv \int_0^1 \sqrt{f(\eta)} d\eta = \sqrt{3/8} \left[\sqrt{4\alpha} + (1 + 4\alpha) \sin^{-1}(1/\sqrt{1 + 4\alpha}) \right] / \sqrt{1 + 6\alpha} \quad (34)$$

and E_σ , for a given value of α , is a constant. Equation (31) indicates that $E_1 = 2E_2$. Tabulated values of the first five roots of (31) for a number of values of E_σ are given in [6]. The values of I_1 for any given slip velocity ratio u_s/\bar{u} are shown in Fig. 4.

The first four eigenvalues and coefficients are shown in table I(a) for symmetrical two-sided heating ($\sigma = 2$) or in table I(b) for unsymmetrical one-sided heating ($\sigma = 1$). The results for continuum flow were obtained from expressions presented in [3], while for slug flow, the eigenvalues were obtained as the positive roots of $\sin \lambda_m^{1/2} = 0$ or $\lambda_m^{1/2} = m\pi$. The coefficients D_m were obtained from the equally simple result $D_m = -2/\lambda_m$.

The numerical value of $1/3$ for u_s/\bar{u} corresponds to $\xi_u/2L = 0.0833$, while a value of $3/5$ for u_s/\bar{u} corresponds to $\xi_u/2L = 0.25$. The results for $u_s/\bar{u} = 1$ (slug flow) are outside the slip regime but have been included as limiting values and for comparison.

The level of accuracy of the foregoing results was checked [4] by computing the eigenvalues and eigenfunctions of (30a), as well as the coefficients C_m given by (16), on an electronic (IBM 7094) computer, by the Runge-Kutta method, for $u_s/\bar{u} = 1/3$ and $3/5$. The eigenvalues and coefficients so obtained are listed in table I. The relevant quantities

as computed from the previously presented analytical expressions are in remarkably close agreement with the electronically computed values, especially for values of $m \geq 2$. It is concluded that the asymptotic formulas are suitable for $m \geq 2$.

The variation of the dimensionless wall-to-bulk temperature difference along the ducts can be evaluated with the numerical information given in table I. Before proceeding with the evaluation, however, it is illuminating to examine the wall-to-bulk temperature difference at the entrance of the heated section. With $x = 0$, (25) becomes

$$(t_w - t_b)_0 / (t_w - t_b)_d = \left[G(1) + \sigma(\xi_t/2L) + \sum_{m=1}^{\infty} C_m R_m(1) \right] / \left[G(1) + \sigma(\xi_t/2L) \right] \quad (35)$$

When $\eta = 1$, however, (15) becomes

$$G(1) = - \sum_{m=1}^{\infty} C_m R_m(1)$$

so that

$$(t_w - t_b)_0 / (t_w - t_b)_d = \sigma(\xi_t/2L) / \left[G(1) + \sigma(\xi_t/2L) \right] \quad (36)$$

In the absence of a temperature-jump effect, the wall-to-bulk temperature difference is zero at the entrance. With a temperature jump, however, the entrance temperature difference has a nonzero value. Equation (36) is plotted in Fig. 5 as a function of the two parameters u_s/\bar{u} and $\xi_t/2L$ for $\sigma = 2$ and 1. For either wall heating situation the entrance temperature difference increases with an increasing value of $\xi_t/2L$.

The magnitude of the slip velocity has only a small influence on the quantity $(t_w - t_b)_0 / (t_w - t_b)_d$ for $\sigma = 1$, while for $\sigma = 2$ the influence of slip velocity is more pronounced.

The variation of the wall-to-bulk temperature difference along the duct length was evaluated from (25) for several values of the rarefaction parameters u_s/\bar{u} and $\xi_t/2L$. Plots are given in Figs. 6 and 7 for $\sigma = 2$ and $\sigma = 1$, respectively.

Inspection of Figs. 6 and 7 reveals several interesting trends. First of all, for a fixed value of $\xi_t/2L$, the wall temperature variation is more sensitive to the slip velocity over most of the duct length for the unsymmetrically heated channel ($\sigma = 1$) than for the symmetrically heated channel ($\sigma = 2$). Near the entrance, however, the reverse effect is obtained. For both wall heating situations, the slip velocity has the effect of retarding $t_w - t_b$ in its approach to the fully developed value, while the temperature jump has the opposite effect. Finally, the abscissa scale for $\sigma = 1$ is twice that for $\sigma = 2$. The length required for the wall-to-bulk temperature difference to approach fully developed conditions is thus greater for the unsymmetrically heated channel than for the channel heated uniformly from both walls.

It is the practice to define a thermal entrance length as the heated length required for $t_w - t_b$ to approach within 5 percent of the fully developed value. A horizontal dashed line corresponding to an ordinate of 0.95 is shown in Figs. 6 and 7.

It is perhaps somewhat more illuminating to present the variation of the wall-to-bulk temperature difference in terms of the rarefaction parameter $\mu\sqrt{R_g t}/2pL$ as in Fig. 8. The effect of increased gas rarefaction is to shorten the thermal entrance length. The accommodation coefficient also has an important effect on the thermal entrance length, and this effect is associated with the increase in temperature jump with

decreased accommodation coefficient.

The longitudinal variation of the Nusselt number along the duct with uniform heat flux at one or both walls (26) was evaluated and is plotted in Fig. 9. The velocity and temperature jumps give rise to opposite changes in their effect on the Nusselt number variation; the velocity jump tends to increase the Nusselt number at a given axial position, while the temperature jump tends to decrease the Nusselt number. Numerical evaluations of the Nusselt number dependence on the parameters $\mu\sqrt{R_g t}/2pL$ and a are plotted in Fig. 10. Clearly the overall effect of the gas rarefaction is always to decrease the Nusselt number below its continuum value at every position along the heated length.

FLOW IN CIRCULAR TUBE

Attention is now turned to the case of axially symmetric slip flow in a circular tube. The coordinate system for the present problem is shown in Fig. 11.

It is again assumed that the velocity profile is fully developed and is unchanging along the tube length. The velocity distribution and the fully developed heat-transfer characteristics have already been investigated for the circular-tube case [1], and many results obtained are immediately applicable. The development of the round-tube system is similar to that of the parallel-plate channel.

The differential equation for convective heat transfer is now

$$\rho C_p u (\partial t / \partial x) = (\kappa / r) (\partial / \partial r) (r \partial t / \partial r) \quad (37)$$

The assumptions and restrictions of this equation are the same as those previously explained. When written in terms of the dimensionless vari-

ables, (37) becomes

$$2\psi f(\omega) (\partial t / \partial \xi) = (1/\omega) (\partial / \partial \omega) (\omega \partial t / \partial \omega) \quad (38)$$

The velocity distribution u is given in [1] and from the results the dimensionless velocity profile $f(\omega)$ and the slip velocity ratio u_s/\bar{u} are easily obtained:

$$f(\omega) = 2(1 - \omega^2 + 4\alpha)/(1 + 8\alpha) \quad \alpha \equiv \xi_u/d \quad (39)$$

$$u_s/\bar{u} = f(1) = 8\alpha/(1 + 8\alpha) \quad (40)$$

For large x , a fully developed temperature profile t_d exists in the form

$$(t_d - t_1)/(qr_0/k) = (4/RePr)(x/r_0) + H(\omega) \quad (40)$$

where the radial function $H(\omega)$ is given in [1] as

$$H(\omega) = \omega^2 - (1/4)\omega^4 - (7/24) - \left[(1/2)\omega^2 - (1/4)\omega^4 \right] (u_s/\bar{u}) + (1/24)(u_s/\bar{u})^2 \quad (41)$$

The solution for the thermal entrance region can be shown to have the form

$$t_e/(qr_0/k) = \sum_{n=1}^{\infty} C_n R_n(\omega) \exp[-4\lambda_n(x/r_0)/RePr] \quad (42)$$

where λ_n and R_n are, respectively, the eigenvalues and eigenfunctions of the Sturm-Liouville problem:

$$\begin{aligned} (d/d\omega)[\omega(dR/d\omega)] + 2\lambda\omega f(\omega)R &= 0 \\ dR/d\omega &= 0 \quad \text{at } \omega = 0, 1 \end{aligned} \quad (43)$$

The coefficients C_n in (42) are obtained from the result

$$\begin{aligned} C_n &= - \int_0^1 2\omega H(\omega) f(\omega) R_n(\omega) d\omega / \int_0^1 2\omega f(\omega) R_n^2(\omega) d\omega \\ &= \int_0^1 2\omega H(\omega) f(\omega) R_n(\omega) d\omega / [R(\omega) (\partial^2 R / \partial \omega \partial \lambda)]_{\omega=1}^{\lambda=\lambda_n} \end{aligned} \quad (44a)$$

or

$$C_n = 1 / [\lambda (\partial^2 R / \partial \omega \partial \lambda)]_{\omega=1, \lambda=\lambda_n} \quad (44b)$$

In order to obtain (44a), the result

$$H(\omega) = - \sum_{n=1}^{\infty} C_n R_n(\omega)$$

was used.

The complete solution for the temperature that applies along the entire tube length is obtained by summing (40) and (42) to obtain

$$(t - t_1) / (qr_0 / \kappa) = 4(x / r_0) / \text{RePr} + H(\omega) + \sum_{n=1}^{\infty} C_n R_n(\omega) \exp[-4\lambda_n(x / r_0) / \text{RePr}] \quad (46)$$

The temperature-jump effect at the tube wall is given by

$$t_g - t_w = -2(qr_0 / \kappa)(\xi_t / d) \quad (47)$$

Hence, the wall temperature along the length of the tube is obtained as

$$(t_w - t_1) / (qr_0 / \kappa) = 4(x / r_0) / (\text{RePr}) + H(1) + 2(\xi_t / d) + \sum_{n=1}^{\infty} C_n R_n(1) \exp[-4\lambda_n(x / r_0) / (\text{RePr})] \quad (48)$$

This equation can be rephrased in terms of the bulk temperature $t_b(x)$

with the result

$$(t_w - t_b) / (t_w - t_b)_d = \left\{ H(1) + 2(\xi_t / d) + \sum_{n=1}^{\infty} C_n R_n(1) \exp[-4\lambda_n(x / r_0) / \text{RePr}] \right\} / [H(1) + 2(\xi_t / d)] \quad (49)$$

where

$$(t_w - t_b)_d = (qr_0 / \kappa) [H(1) + 2(\xi_t / d)] \quad (50)$$

and

$$t_b(x) = t_1 + (qr_0 / \kappa)(4x / r_0) / \text{RePr} \quad (51)$$

The Nusselt number may be determined from the definition

$$\text{Nu} \equiv h(2r_0)/\kappa = [q/(t_w - t_b)](2r_0/\kappa) \quad (52)$$

When (49) and (50) are used, the result obtained is

$$\text{Nu} = 2 \left\{ H(1) + 2(\xi_t/d) + \sum_{n=1}^{\infty} C_n R_n(1) \exp \left[-4\lambda_n(x/r_0)/\text{RePr} \right] \right\} \quad (53)$$

The Nusselt numbers at the entrance of the heated section Nu_0 and in the fully developed region Nu_d are readily obtained from (53) as

$$\text{Nu}_0 = 1/(\xi_t/d) \quad (54)$$

$$\text{Nu}_d = (48/11) / [1 - (6/11)(u_s/\bar{u}) + (1/11)(u_s/\bar{u})^2 + (48/11)(\xi_t/d)] \quad (55)$$

The effects of gas rarefaction on the fully developed Nusselt number (55) have been considered in [1].

The asymptotic behavior of (43) at large values of λ is examined in [4,7] and it is shown that the asymptotic expressions for the eigenvalues λ_n and constants $D_n \equiv C_n R_n(1)$ are given by

$$\tan \beta_n = \frac{M\beta_n + N}{M\beta_n - N} \quad (56)$$

$$D_n = -16\alpha / [N + (N^2/M) + M\beta_n^2] \quad (57)$$

where

$$\beta_n \equiv \sqrt{\lambda_n} \tilde{I}_1 \quad (58)$$

$$\tilde{I}_1 \equiv \int_0^1 \sqrt{2f(\omega)} d\omega = [\sqrt{4\alpha} + (1 + 4\alpha)\sin^{-1}(1/\sqrt{1 + 4\alpha})] / \sqrt{1 + 8\alpha} \quad (59)$$

$$M \equiv 4(4\alpha)^{3/2} / [\sqrt{4\alpha} + (1 + 4\alpha)\sin^{-1}(1/\sqrt{1 + 4\alpha})] \quad (60)$$

$$N \equiv 1 - 4\alpha \quad (61)$$

The values of \tilde{I}_1 for any given slip velocity ratio u_s/\bar{u} are shown in Fig. 12.

The first four eigenvalues and coefficients for the case of flow in a round tube are shown in table II. The results for continuum flow ($u_s/\bar{u} = 0$) were obtained from expressions given by Dzung [8], while for slug flow ($u_s/\bar{u} \rightarrow 1$) the eigenvalues were obtained as the roots of $J_1(2\lambda_n)^{1/2} = 0$. The coefficients D_n are then obtained from the simple result $D_n = -1/\lambda_n$. Also shown in table II are the data obtained through the use of an IBM 7094 computer by the Runge-Kutta method [4]. It is apparent that the asymptotic formulas yield values of sufficient accuracy for $n \geq 2$.

Numerical values of the Nusselt number variation along the tube length (53) were evaluated as functions of the two parameters u_s/\bar{u} and ξ_t/d and are plotted in Fig. 13. The trends are similar to those observed in the parallel-plate channel system. The Nusselt number variation can be calculated as a function of the parameter $\mu\sqrt{R_g t}/pd$; the results of such a calculation are plotted in Fig. 14. Increased gas rarefaction and/or decreased accommodation coefficient reduces the Nusselt number below its continuum value, and, in addition, shortens the thermal entrance length, which has been defined alternatively as the heated length required for the Nusselt number to approach within 5 percent the fully developed value as given by (55).

OTHER RAREFACTION EFFECTS

In [4], modification of the present heat-transfer results for laminar channel or tube slip flow is made, or discussed, to account for additional slip effects, such as wall shear work, modified temperature jump, and thermal creep velocity.

CONCLUSIONS

Solutions were obtained for laminar, forced-convection heat transfer to a slightly rarefied gas flowing between parallel plates or in a circular tube with uniform wall heat flux. The wall temperatures and Nusselt numbers in the entrance and fully developed regions can be obtained as functions of the velocity and temperature jumps at the wall, or as functions of the mean free path.

The results indicate that the slip-flow Nusselt numbers are lower than those for continuum flow at all axial locations along the conduits and also that the thermal entrance length is decreased with increased gas rarefaction for either the parallel-plate channel or the circular tube.

REFERENCES

1. Sparrow, E. M., and Lin, S. H.: Laminar Heat Transfer in Tubes Under Slip-Flow Conditions. J. Heat Transfer (Trans. ASME, Series C), vol. 84, no. 4, Nov. 1962, pp. 363-369.
2. Deissler, R. G.: An Analysis of Second-Order Slip Flow and Temperature Jump Boundary Conditions for Rarefied Gases. Int. J. Heat Mass Transfer, vol. 7, no. 6, June 1964, pp. 681-694.
3. Dzung, L. S.: Heat Transfer in a Flat Duct with Sinusoidal Heat Flux Distribution. Proc. Second U.N. Conf. on Peaceful Uses of Atomic Energy (Geneva), vol. 7, United Nations, Geneva, 1958, pp. 671-675.
4. Inman, R. M.: Laminar Slip Flow Heat Transfer in a Parallel-Plate Channel or a Round Tube with Uniform Wall Heating. NASA TN D-2393, 1964.
5. Chambre, P. L., and Schaaf, S. A.: Flow of Rarefied Gases. Princeton University Press, Princeton, N.J., 1961.

6. Carslaw, H. S., and Jaeger, J. C.: Conduction of Heat in Solids, Second edition, Oxford University Press, London, 1959, p. 491.
7. Inman, R. M.: Approximation of the Eigenvalues for Heat Transfer in Laminar Tube Slip Flow, AIAA Jour., vol. 2, no. 2, Feb. 1964, pp. 373-374.
8. Dzung, L. S.: Heat Transfer in a Round Duct with a Sinusoidal Heat Flux Distribution. Proc. Second U.N. Conf. on Peaceful Uses of Atomic Energy (Geneva), vol. 7, United Nations, Geneva, 1958, pp. 657-670.

TABLE I. - EIGENVALUES AND COEFFICIENTS FOR SLIP FLOW IN A
PARALLEL-PLATE CHANNEL WITH UNIFORM HEAT FLUX

(a) Symmetry number, 2.

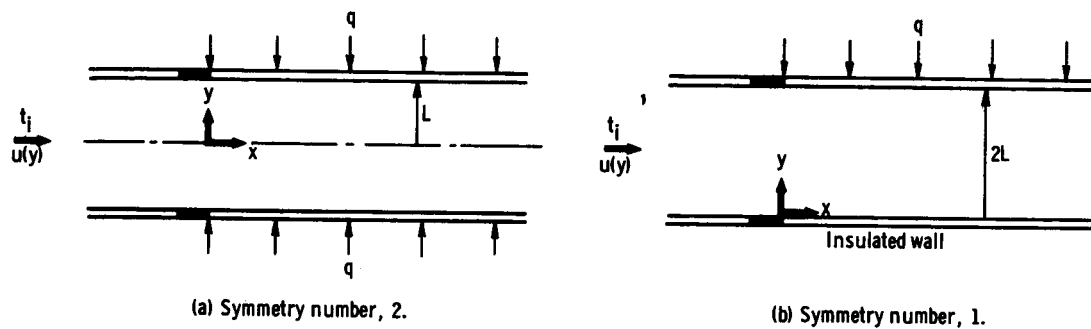
	Ratio of slip to average velocity, u_s/\bar{u}					
	0	1/3		3/5		1
		Analytical solution	Numerical solution, Runge-Kutta method	Analytical solution	Numerical solution, Runge-Kutta method	
Eigenvalue						
$\lambda_1^{1/2}$	3.540	3.78	3.33	3.35	3.23	3.14
$\lambda_2^{1/2}$	6.800	6.72	6.49	6.41	6.36	6.28
$\lambda_3^{1/2}$	10.05	9.78	9.65	9.54	9.50	9.42
$\lambda_4^{1/2}$	13.30	12.90	12.82	12.69	12.65	12.56
Coefficient						
D_1	-0.2090	-0.1479	-0.2331	-0.2110	-0.2264	-0.2030
D_2	- .0703	- .0642	- .0701	- .0613	- .0618	- .0508
D_3	- .0367	- .0332	- .0336	- .0282	- .0280	- .0226
D_4	- .0230	- .0198	- .0197	- .0165	- .0161	- .0127

(b) Symmetry number, 1.

	Ratio of slip to average velocity, u_s/\bar{u}					
	0	1/3		3/5		1
		Analytical solution	Numerical solution, Runge-Kutta method	Analytical solution	Numerical solution, Runge-Kutta method	
Eigenvalue						
$\lambda_1^{1/2}$	3.800	4.09	3.50	3.51	3.35	3.14
$\lambda_2^{1/2}$	7.071	6.99	6.66	6.51	6.46	6.28
$\lambda_3^{1/2}$	10.33	10.01	9.82	9.61	9.58	9.42
$\lambda_4^{1/2}$	13.60	13.09	12.98	12.72	12.71	12.56
Coefficient						
D_1	-0.1470	-0.0711	-0.1821	-0.1685	-0.1920	-0.2030
D_2	- .0525	- .0425	- .0583	- .0567	- .0566	- .0508
D_3	- .0278	- .0259	- .0291	- .0271	- .0267	- .0226
D_4	- .0176	- .0169	- .0175	- .0156	- .0154	- .0127

TABLE II. - EIGENVALUES AND COEFFICIENTS FOR SLIP FLOW IN A
CIRCULAR TUBE WITH UNIFORM WALL HEAT FLUX

	0	Ratio of slip to average velocity, u_s/\bar{u}				
		2/5		2/3		1
		Analytical solution	Numerical solution, Runge-Kutta method	Analytical solution	Numerical solution, Runge-Kutta	
Eigenvalue						
$\lambda_1^{1/2}$	2.531	-----	2.55	2.64	2.60	2.710
$\lambda_2^{1/2}$	4.578	4.71	4.63	4.75	4.74	4.955
$\lambda_3^{1/2}$	6.599	6.76	6.69	6.88	6.86	7.195
$\lambda_4^{1/2}$	8.610	8.81	8.75	9.00	8.98	9.425
Coefficient						
D_1	-0.1985	-----	-0.1855	-0.1670	-0.1658	-0.1360
D_2	- .0693	-0.0594	- .0605	- .0515	- .0510	- .0406
D_3	- .0365	- .0306	- .0301	- .0247	- .0245	- .0194
D_4	- .0230	- .0217	- .0185	- .0145	- .0144	- .0113



(a) Symmetry number, 2.

(b) Symmetry number, 1.

Figure 1. - Physical model and coordinate system for parallel-plate channel.

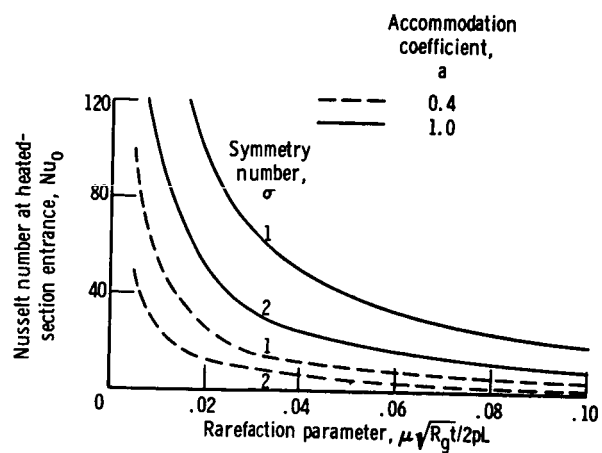


Figure 2. - Effect of gas rarefaction on entrance Nusselt number for parallel-plate channel.

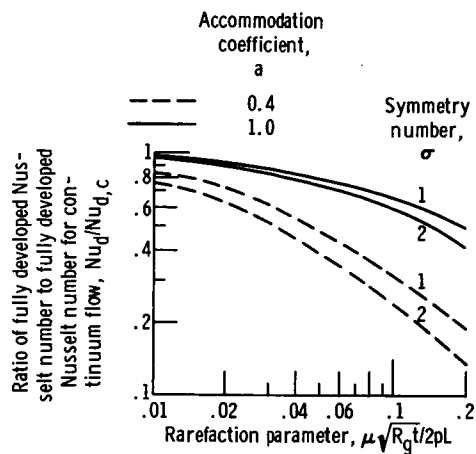


Figure 3. - Fully developed Nusselt number variation in parallel-plate channel with uniform wall heat flux. Specular reflection coefficient, 1; ratio of specific heats, 1.4; Prandtl number, 0.73.

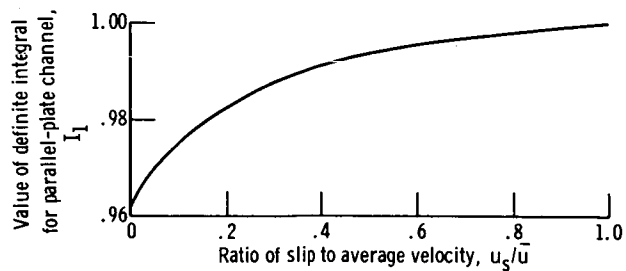


Figure 4. - Value of definite integral for parallel-plate channel for any value of slip to average velocity ratio.

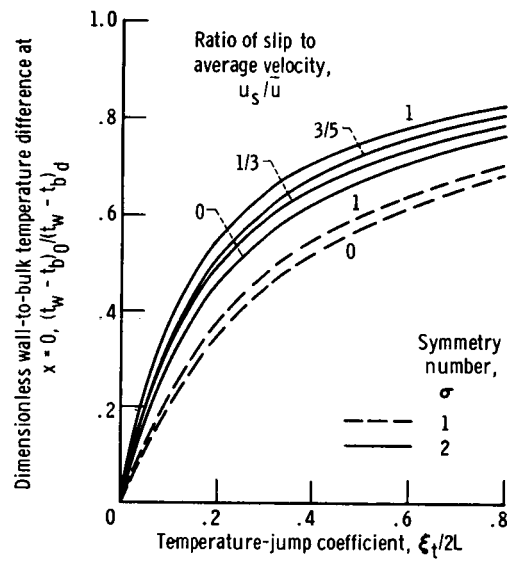


Figure 5. - Variation of dimensionless wall-to-bulk temperature difference at heated section entrance for slip flow in parallel-plate channel with uniform wall heat flux.

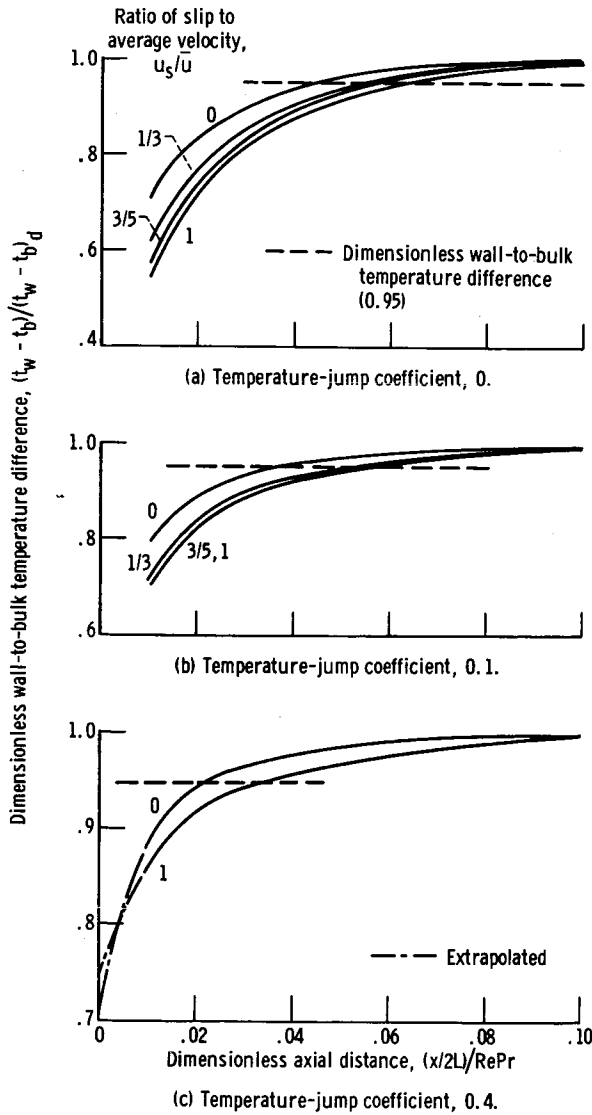


Figure 6. - Wall temperature ratio in thermal entrance region for flow in parallel-plate channel with uniform wall heat flux and different values of temperature-jump coefficient. Symmetry number, 2.

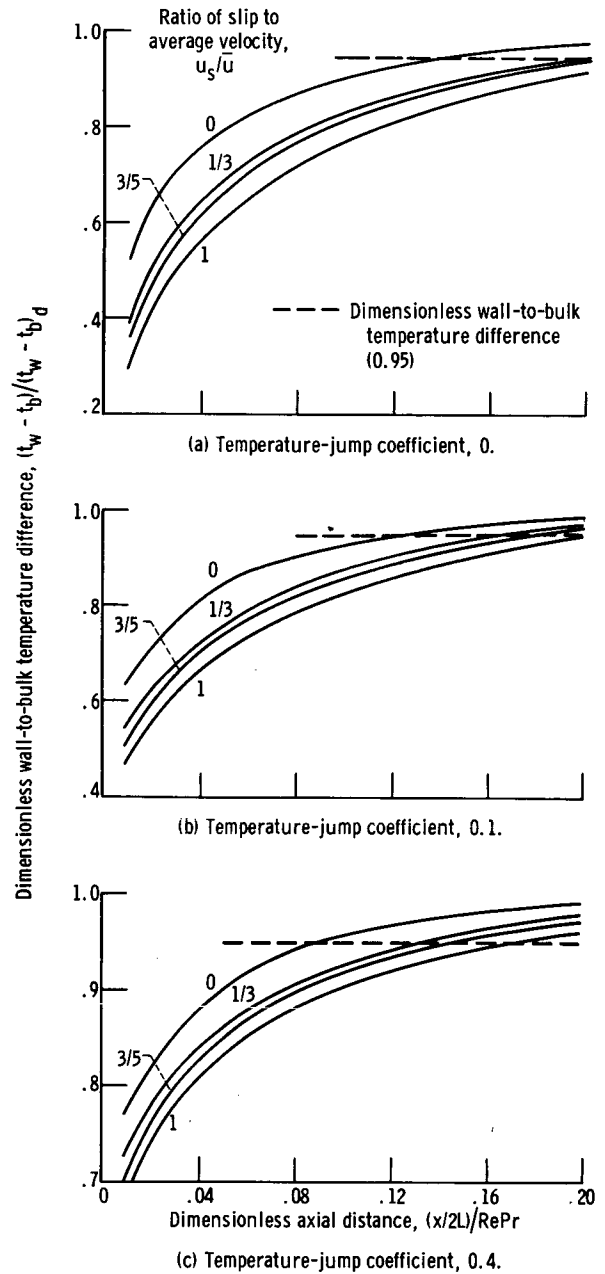


Figure 7. - Wall temperature ratio in thermal entrance region for flow in parallel-plate channel with uniform wall heat flux and different values of temperature-jump coefficient. Symmetry number, 1.

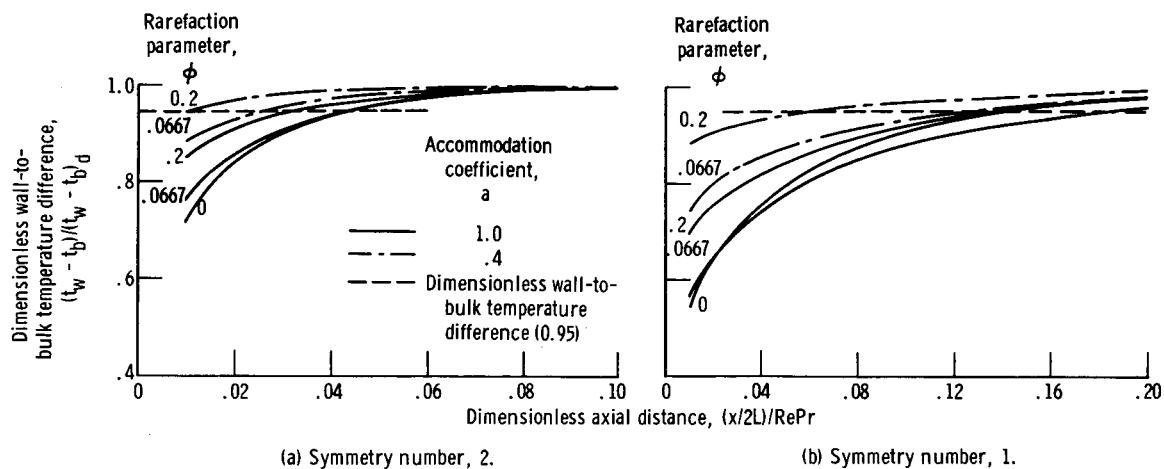


Figure 8. - Wall temperature ratio in thermal entrance region for flow in a parallel-plate channel with uniform wall heat flux. Specular reflection coefficient, 1; ratio of specific heats, 1.4; Prandtl number, 0.73.

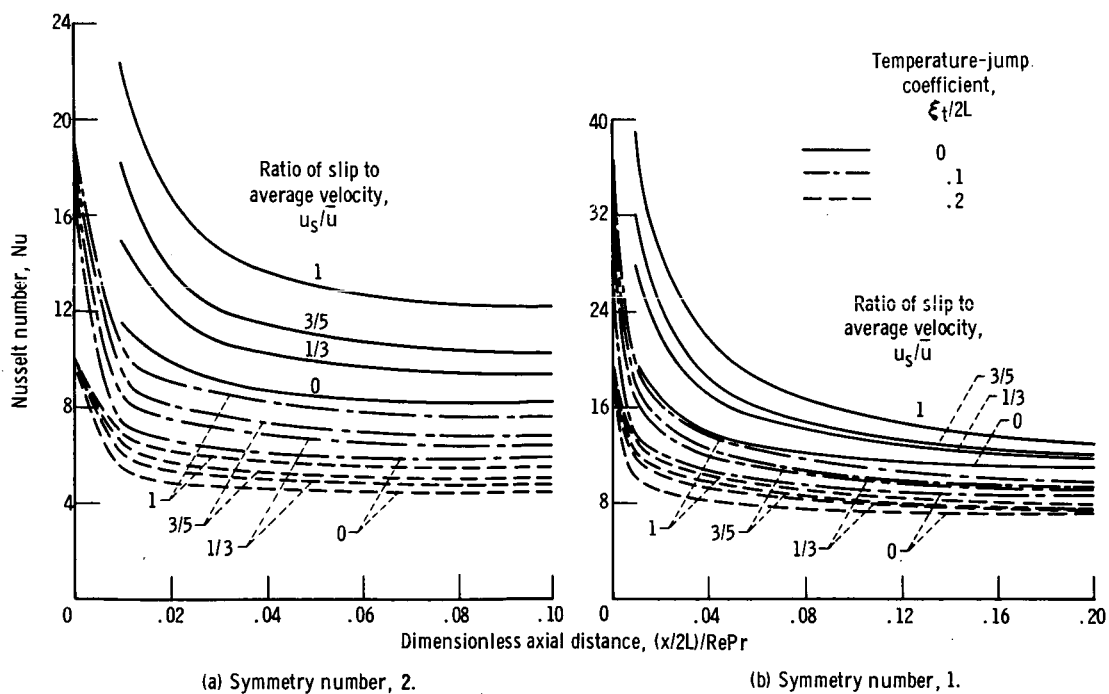


Figure 9. - Variation of Nusselt number along parallel-plate channel for uniform wall heat flux and different values of temperature-jump coefficient.

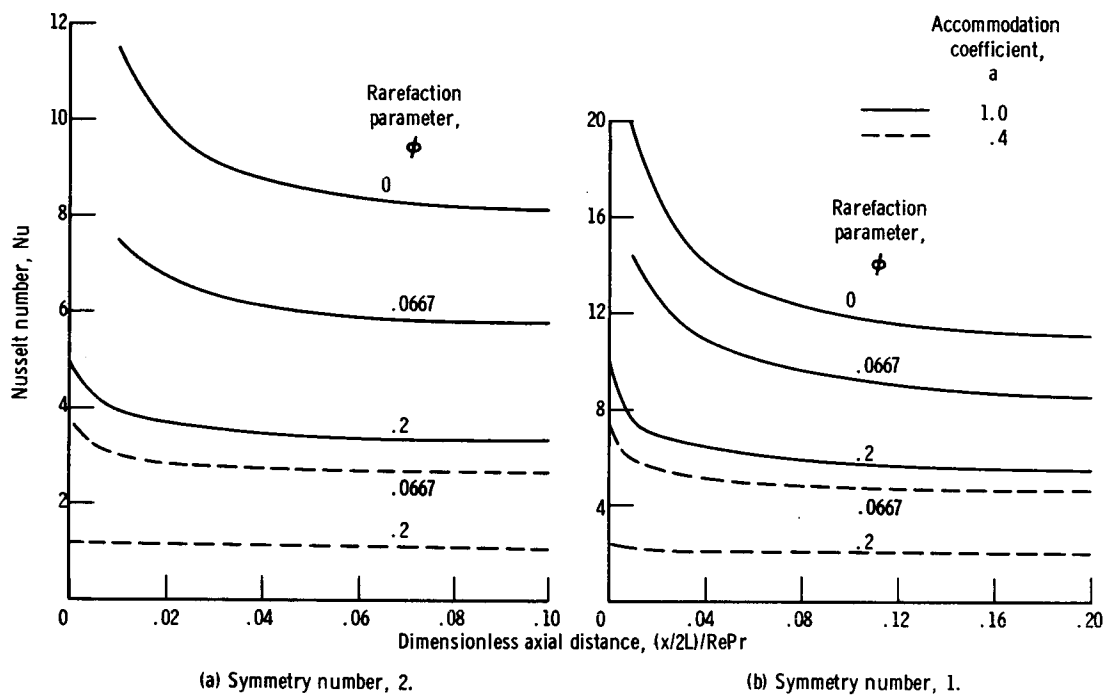


Figure 10. - Variation of Nusselt number along parallel-plate channel for uniform wall heat flux. Specular reflection coefficient, 1; ratio of specific heats, 1.4; Prandtl number, 0.73.

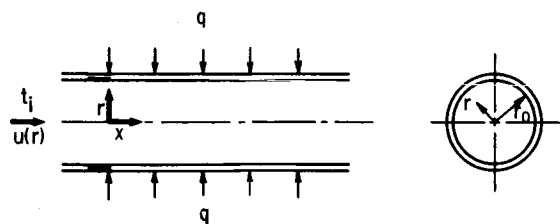


Figure 11. - Physical model and coordinate system for round tube.

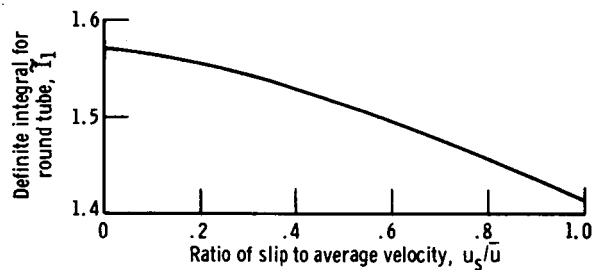


Figure 12 - Values of definite integral for any value of slip to average velocity ratio in round tube.

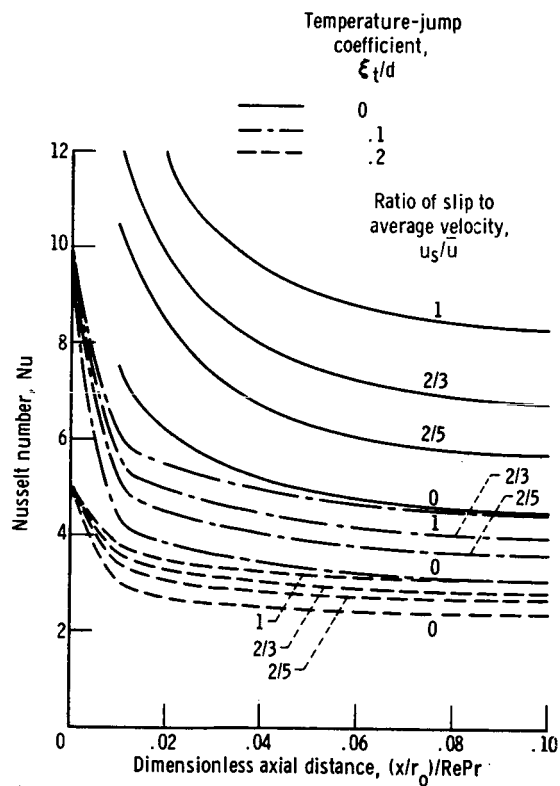


Figure 13. - Variation of Nusselt number along round tube for uniform wall heat flux and different values of temperature-jump coefficient.

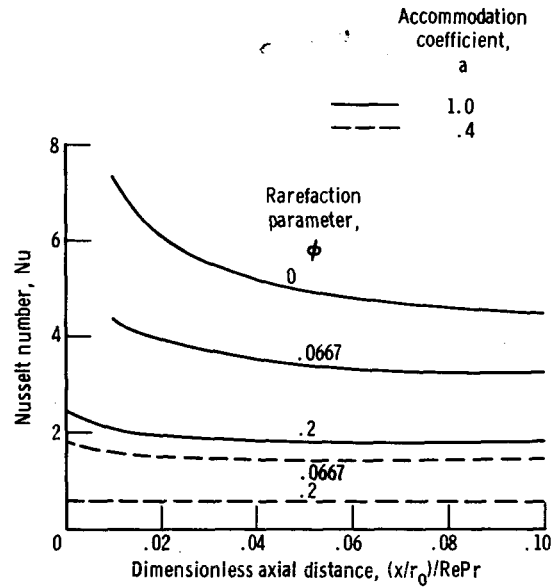


Figure 14. - Variation of Nusselt number along round tube for uniform wall heat flux. Specular reflection coefficient, 1; ratio of specific heats, 1.4; Prandtl number, 0.73.

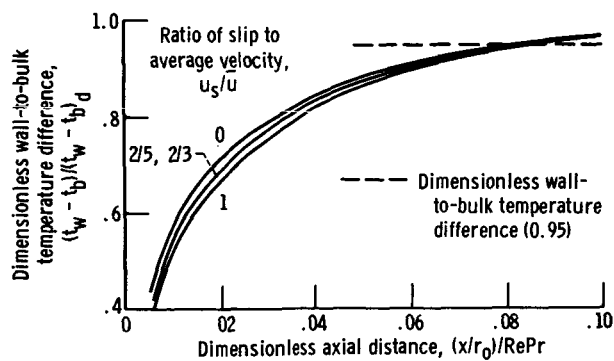


Figure 15. - Wall temperature ratio in thermal entrance region of round tube for uniform wall heat flux and temperature-jump coefficient of zero.